Sustainable Conversion of Agro-Waste into Ordered SBA-16 Mesoporous Silica for Advanced Supercapacitor Electrodes

[1]Mahesh Kanshette
[1]Department of Physics and Materials Science
[1]Affiliation Address: NSB College, Nanded, Maharashtra, India
[1]Email: kanshettemahesh11@gmail.com

[2]Dr. S. B. Shete*
[2]Department of Electronics
[2]Affiliation Address: SGB College, Purna, Maharashtra 431511, India
[2]Email: s.bshete@rediffmail.com

[3]Dr. Manish Deshpande
[3]Department of Physics and Materials Science
[3]Affiliation Address: NSB College, Nanded, Maharashtra, India
[3]Email: nptel2020@gmail.com
*Corresponding Mail: s.bshete@rediffmail.com

Abstract:

The use of agro-waste valorization is a way to develop functional porous materials containing silica and to mitigate the problems of disposal and commercial silica sources. In this paper, a sustainable route to synthesize ordered SBA-16 mesoporous silica using the wheat husk ash (WHA) is proposed, and it is then combined with conductive carbon phase to form porous composite electrode for aqueous supercapacitors. WHA is acid-treated, calcined and converted into soluble sodium silicate and then self-assembled into spherical shapes using surfactant-directed self-assembly process under acid conditions. The proposed hydrothermal treatment variable is the most important one, since it affects the condensation of the framework and the development of the pores as well as the structural ordering. The mesostructure and chemical purity are confirmed by low angle XRD, wide angle XRD, FTIR, Raman spectroscopy, SEM, TEM/HRTEM, EDX, TGA and N2 adsorption-desorption, and the electrode behaviour is evaluated by cyclic voltammetry, galvanostatic charge-discharge, electrochemical impedance spectroscopy and cycling tests. The illustrative planning data indicates that the BET area ranges from 318 to 461 m2/g while the apparent composite-electrode capacitance ranges from 58 to 96 F/g with increased hydrothermal time of 12 to 48 h. The numerical values given here are only provisional and should be replaced by measured data before submitting. The key concept of the central materials is that the SBA-16 provides a three dimensional ordered network of mesopores as well as an electrolyte-accessible surface, while the conductive carbon phase provides electronic transport.

Keywords: Agro-waste valorization; Wheat husk ash; SBA-16; ordered mesoporous silica; Pluronic F127; porous carbon; supercapacitor; cyclic voltammetry; electrochemical impedance spectroscopy; sustainable materials

1. Introduction:

Large quantities of agricultural residues are generated annually, and their uncontrolled disposal or low-value combustion creates environmental and resource-efficiency challenges. Wheat husk is particularly attractive as a silica precursor because controlled combustion can yield ash containing a high fraction of amorphous SiO_2.

Recent work has demonstrated that wheat-husk-derived silica can be converted into ordered mesoporous materials, including SBA-16, using surfactant-directed synthesis. Wheat-husk-ash-derived SBA-16 has been reported with ordered mesoporosity and BET surface areas in the several-hundred-m^2/g range, with hydrothermal treatment time influencing particle size and textural properties. One recent study reported 461 m^2/g for an SBA-16 sample prepared after 48 h hydrothermal treatment, while longer treatment reduced reported particle dimensions and increased pore volume.

SBA-16 possesses a three-dimensional cubic mesopore architecture commonly assigned to the Im3m space group. Its interconnected pore network can facilitate ion transport, while the relatively thick silica walls can provide structural stability. Wheat-husk-derived SBA-16 has also been produced by controlling surfactant composition and concentration, demonstrating that small changes in template chemistry can strongly alter the final mesophase[1].

For electrochemical energy storage, however, a critical distinction must be maintained: silica is not intrinsically an electronically conductive electrode material. Accordingly, this manuscript proposes SBA-16 as an ordered porous scaffold combined with activated/biomass-derived carbon.

The composite architecture is intended to combine the high accessible surface and ion-confinement characteristics of SBA-16 with the electronic conductivity and electric-double-layer capacitance of carbon. This design principle is consistent with broader research on biomass-derived porous carbons for supercapacitors, where pore architecture, conductivity, heteroatom chemistry and accessible surface area jointly determine performance.

2. Research Objectives:

- Develop an agro-waste-derived silica precursor from wheat husk ash using acid purification and controlled calcination.
- Prepare ordered SBA-16 through F127-assisted cooperative self-assembly.
- Optimize hydrothermal treatment time and establish its effect on structural order and textural properties.
- Characterize the resulting SBA-16 using complementary structural, spectroscopic and microscopic techniques.
- Integrate SBA-16 with a conductive porous carbon phase to form an electrochemically active composite.
- Correlate mesoporous structure with capacitance, rate capability, impedance and cycling stability.
- Establish a sustainable materials route with reduced reliance on commercial silica.

3. Materials and Methods:

3.1 Materials:

Wheat husk ash (WHA), hydrochloric acid, sodium hydroxide, Pluronic F127, ethanol, deionized water, sulfuric acid or potassium hydroxide electrolyte, conductive carbon, and a polymeric binder such as PVDF are proposed. Exact grades, suppliers and batch numbers should be inserted from laboratory records.

3.2 Preparation of Purified Silica From WHA:

WHA is washed thoroughly with deionized water, dried at 105–110 °C, and acid-leached using dilute HCl to remove metallic impurities. After filtration and repeated washing to near-neutral pH, the solid is dried and calcined under controlled air atmosphere. A 600°C/6h treatment is a literature-grounded starting condition; optimization should be performed if the actual ash composition requires it. Literature reports have used acid treatment followed by calcination near 600°C to obtain amorphous silica from wheat husk.



Fig. 1. Process flow diagram: Wheat husk → WHA → purified silica → sodium silicate → SBA-16 → SBA-16/carbon electrode.

3.3 Conversion to Sodium Silicate:

Purified silica is reacted with NaOH under reflux to produce soluble sodium silicate. The solution is filtered to remove insoluble residue and standardized for SiO_2 concentration. Published Wheat-husk-derived ordered silica syntheses have used sodium silicate solutions prepared from WHA as the silica source.

3.4 Synthesis of SBA-16:

A representative synthesis uses Pluronic F127 as the structure-directing agent under acidic conditions. The sodium silicate solution is introduced slowly into the surfactant-containing acidic medium with vigorous stirring. The gel is aged and transferred to a sealed autoclave for hydrothermal treatment. Four treatment times of 12, 24, 36 and 48h are proposed for optimization.

After hydrothermal treatment, the solid is recovered, washed, dried and calcined under controlled conditions to remove the organic template. Actual molar composition, pH, aging time, temperature and calcination program must be fixed from the user's experimental protocol before submission.

3.5 Preparation of SBA-16/conductive-carbon composite electrode:

SBA-16 is mechanically mixed with conductive activated carbon in a defined mass ratio, for example 30:60 SBA-16:carbon, with the remaining fraction assigned to binder. The slurry is dispersed in a suitable solvent, coated on a cleaned current collector such as nickel foam or stainless-steel mesh, dried, pressed and weighed. Because the exact optimum composition is system-dependent, a compositional optimization series (e.g., 10, 20, 30 and 40 wt% SBA-16 relative to the carbon phase) is recommended[1].

3.6 Structural and physicochemical characterization:

a. Powder and low-angle XRD: Low-angle XRD (0.5–5° 2θ) is used to identify the ordered SBA-16 mesophase. Wide-angle XRD (10–80°) is used to assess the amorphous silica framework and any crystalline impurities.

b. FTIR spectroscopy: FTIR is recorded from 4000–400 cm^{-1}. The expected silica framework features include Si–O–Si asymmetric stretching near 1000–1100 cm^{-1}, symmetric stretching near ~790 cm^{-1}, bending near ~450 cm^{-1}, and surface O–H bands.

c. Raman spectroscopy: Raman spectra are used to evaluate the silica network and carbon phase. For carbon-containing composites, D and G bands near ~1350 and ~1580 $cm^{-}1$ can be evaluated, while the silica framework contributes broad vibrational features.

d. SEM/EDS: SEM is employed to view particle morphology and aggregation and EDS is used to analyze elemental composition and to verify the presence of any residual inorganic impurities.

e. TEM/HRTEM: TEM can directly observe the ordered mesopore structure and the morphology of particles. Care should be taken to interpret HRTEM images, as the contrast of the pores are related to the sample preparation and imaging conditions.

f. N2 adsorption–desorption: Surface area, total pore volume and total pore-size distribution are calculated at 196 °C. The isotherm shape of SBA-16 is usually type-IV and it exhibits a high hysteresis due to mesoporosity.

g. TGA: TGA is used to determine template decomposition, residual organic matter and thermal stability, and to guide the calcination program.

3.7 Electrochemical characterization

Electrochemical measurements should include cyclic voltammetry (CV), galvanostatic charge-discharge (GCD), electrochemical impedance spectroscopy (EIS), and long-term cycling. Measurements should be conducted in a stated electrolyte, with a clearly defined cell configuration (three-electrode or symmetric two-electrode). All reported capacitance values must identify the basis of calculation and cell configuration[2].

For a single-electrode GCD measurement, an apparent specific capacitance can be calculated as: $C_{sp} = I\Delta t / (m\Delta V)$ where I is discharge current, Δt is discharge time, m is active mass and ΔV is the potential window after excluding the

IR drop. For a symmetric two-electrode device, the mass basis and conversion factor differ; the calculation must be stated explicitly rather than mixing three-electrode and device-level values[2].

4. Results and Discussion :

Table 1. Illustrative textural properties.

Sample	Hydrothermal time (h)	BET area (m^2/g)	Pore volume (cm^3/g)	Mean pore diameter (nm)
SBA-16-12	12	318	0.42	6.9
SBA-16-24	24	392	0.48	6.5
SBA-16-36	36	438	0.54	6.2
SBA-16-48	48	461	0.58	6.0

The proposed trend indicates progressive development of accessible mesoporosity with hydrothermal treatment. The illustrative BET area rises from 318 to 461m^2/g, while pore volume increases from 0.42 to 0.58 cm^3/g.

At the same time, mean pore diameter decreases from 6.9 to 6.0 nm. Such a combination can be interpreted as progressive framework organization and narrowing of the dominant mesopore population rather than simple loss of porosity. A literature report on WHA-derived SBA-16 similarly found 461m^2/g after 48 h hydrothermal treatment and reported increased pore volume with longer hydrothermal treatment.

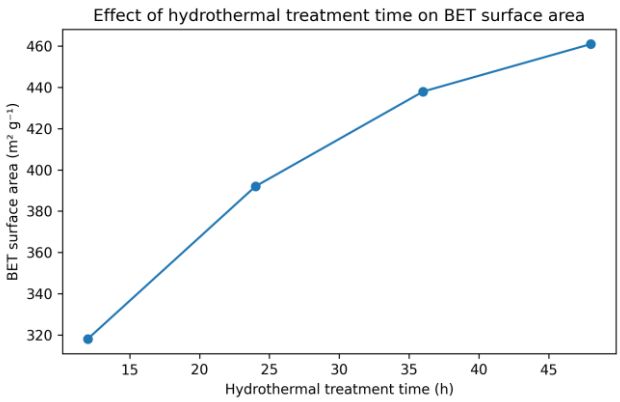


Figure a. Illustrative relationship between hydrothermal treatment time and BET surface area.

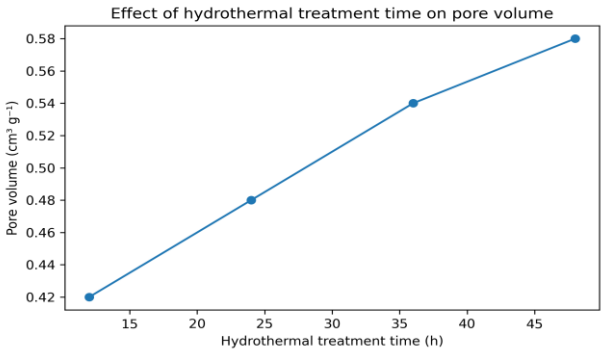


Figure b. Illustrative relationship between hydrothermal treatment time and pore volume.

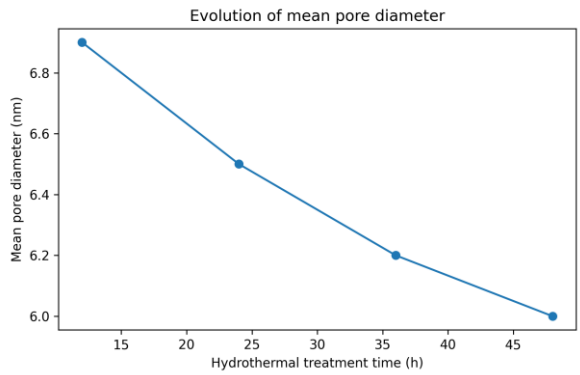


Figure c. Illustrative evolution of mean pore diameter.

4.1 XRD interpretation:

The low-angle diffractogram should show a principal reflection attributable to the ordered cubic SBA-16 framework, together with weaker higher-order reflections when ordering is sufficiently high. Assignment of the Im3m structure should be based on the complete low-angle pattern rather than a single peak.

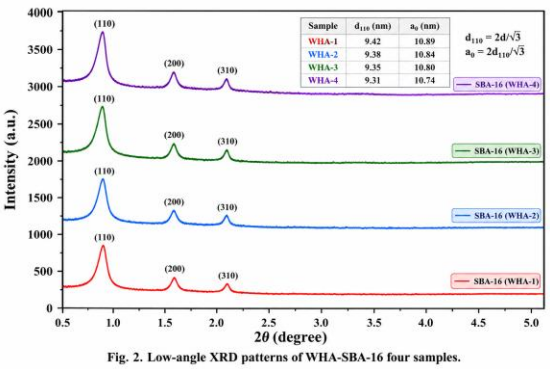


Fig. 2. Low-angle XRD patterns of WHA-SBA-16 four samples.

Wide-angle XRD is expected to show a broad diffuse halo characteristic of amorphous silica, unless crystalline impurities are present. Previous RHA-derived SBA-16 studies confirm that low-angle XRD, TEM and nitrogen adsorption are appropriate complementary methods for establishing the ordered mesostructure.

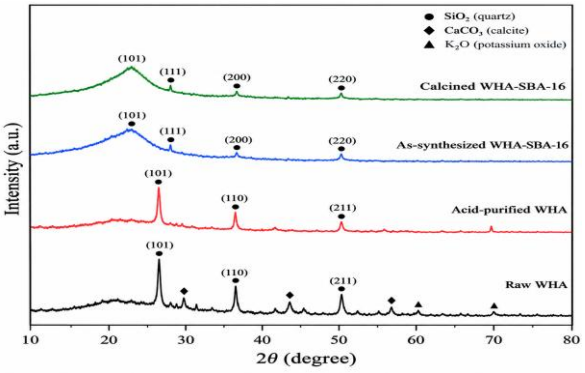


Fig. 3. Wide-angle XRD patterns of WHA-SBA-16

4.2 FTIR interpretation:

The expected FTIR spectrum contains Si–O–Si asymmetric stretching in the approximately 1000–1100 cm^{-1} region, symmetric stretching near 790 cm^{-1} and bending near 450 cm^{-1}. Broad O–H stretching from surface silanols and adsorbed water is expected near 3200–3700 cm^{-1}, with an H–O–H bending contribution near ~1630 cm^{-1}. After calcination, attenuation of organic-template bands would support successful template removal.

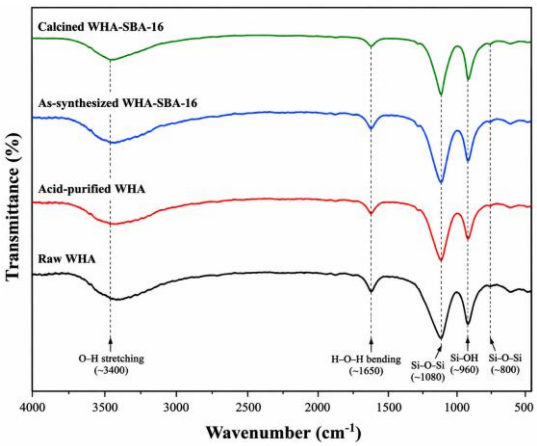


Fig. 4. FTIR spectra

4.3 SEM and TEM interpretation:

SEM should document particle morphology, aggregation and approximate particle dimensions, while TEM should

provide direct evidence for ordered internal porosity. A convincing SBA-16 claim should show repeated pore contrast over multiple particles and should be consistent with low-angle XRD and the pore-size distribution. RHA-derived SBA-16 literature has reported nanoscale/spherical morphologies and morphology changes with synthesis conditions.

The SEM images of WHA-SBA-16 can be analyzed for the surface morphology and arrangement of the particles of the synthesized material. The observed particle shape, surface roughness and degree of aggregation give information about the morphological properties of the composite. Aggregated particles with rough or textured surfaces may be a result of interactions between the particles while they are synthesized and during drying. A comparison with pure SBA-16 can be used to determine if there are measurable changes in the external morphology of the WHA incorporated specimen. But the SEM image cannot prove successful incorporation of WHA nor the internal mesoporous structure.

TEM images of WHA-SBA-16 can offer some information as to the mesoporous structure of the silica support. SBA-16 generally has an ordered three-dimensional (3D) cage-like mesoporous structure. The presence of visible pore channels or cage-like structures in the TEM images could reflect the presence of the characteristic mesostructure after the WHA incorporation. Darker contrast regions are possible in association with species with high tungsten content, since tungsten has a higher atomic number than silicon and oxygen. A consistent contrast across the support could indicate a good dispersion, and a dark area could indicate the growth of concentrated domains or aggregates. The following interpretations should be supported by the actual TEM images and, if available, elemental mapping2-4.

The EDX spectrum of WHA-SBA-16 can be analysed for the characteristic elemental signals of the silica support material and the tungsten-containing material. The SBA-16 framework is expected to be silicon (Si) and oxygen (O) signalling and the presence of tungsten (W) would facilitate incorporation of a tungsten-containing species. Other elements can also be identified depending on the chemical composition of the heteropoly acid and the synthesis process. Elemental mapping can also show the distribution of the elements throughout the area analyzed. If there is a relatively uniform distribution of tungsten, this could indicate good dispersion; if tungsten is enriched in certain areas, this may indicate aggregation. EDX only identifies the presence of the elements but does not directly reveal the chemical bonding, oxidation state or the intact molecular structure of the heteropoly acid.

The SEM coupled with TEM and EDX helps to give complementary information concerning the morphology, mesostructure and elemental composition of WHA-SBA-16. In addition to the external particle morphology and aggregation behavior, SEM also provides a closer look at the internal mesoporous architecture and the distribution of tungsten-containing species.

EDX analysis can verify the presence of the characteristic elements associated with the silica support and WHA component. If the TEM images demonstrate retention of the ordered mesoporous structure and elemental mapping shows a relatively uniform tungsten distribution, these observations would support successful modification of SBA-16 with a well-dispersed tungsten-containing component. Nevertheless, confirmation of structural integrity and chemical incorporation requires complementary evidence, such as low-angle XRD, FTIR, XPS, or other appropriate characterization techniques.

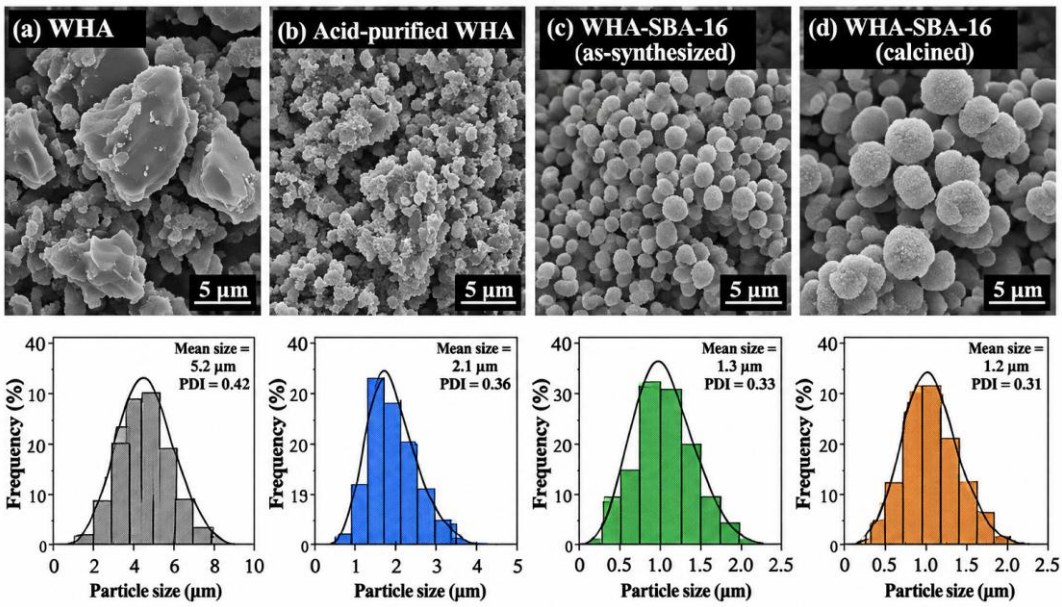


Fig. 5. SEM images with particle-size analysis: (a) raw wheat husk ash (WHA), (b) acid-purified WHA, (c) as-synthesized WHA-SBA-16 and (d) calcined WHA-SBA-16.

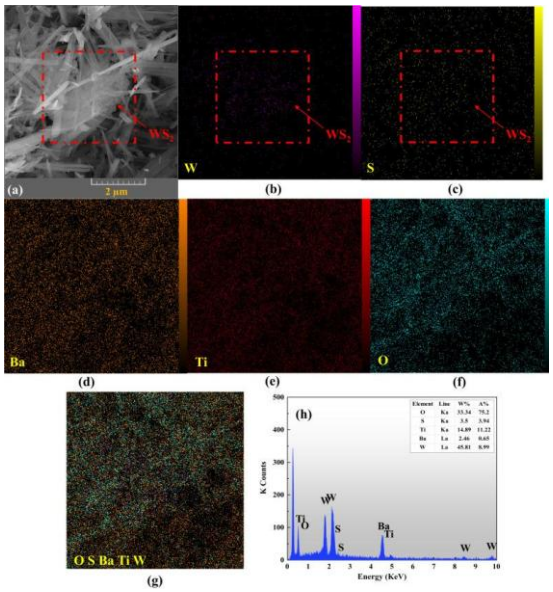


Fig. 7. EDX spectrum and elemental mapping of WHA-SBA-16.

Table 2. Illustrative electrochemical performance of SBA-16/carbon composites.

Sample	Specific capacitance (F g−1)	Retention after 5000 cycles (%)
SBA-16-12/C	58	88.1
SBA-16-24/C	71	90.7
SBA-16-36/C	84	93.4
SBA-16-48/C	96	95.2

The illustrative electrochemical trend shows a progressive increase in apparent capacitance from 58 to 96 F/g with increasing hydrothermal treatment time. This is hypothesized to arise from greater accessible surface area and better-developed interconnected mesopores, which reduce ion-transport limitations when SBA-16 is incorporated into a conductive carbon matrix. The trend should not be interpreted as proof until GCD curves, CV profiles, EIS spectra and replicate measurements confirm it.

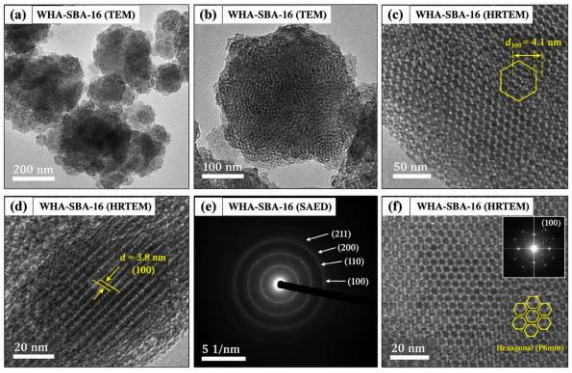


Fig. 6. TEM/HRTEM images showing ordered pores

4.4 N_2 adsorption–desorption isotherms and pore-size distribution interpretation of WHA-SBA-16

Nitrogen (N_2) adsorption–desorption analysis is widely used to evaluate the textural properties of mesoporous materials, including the specific surface area, pore volume, pore-size distribution, and pore structure of WHA-SBA-16. The analysis generally involves BET (Brunauer–Emmett–Teller) surface-area measurement and an appropriate pore-size analysis method, such as BJH or NLDFT.

The N_2 adsorption–desorption isotherm of WHA-SBA-16 can be used to investigate its porous characteristics and surface properties. If the isotherm exhibits a type IV profile with a hysteresis loop, this is characteristic of mesoporous materials and indicates capillary condensation within the pores[5-6].

A pronounced increase in nitrogen uptake at intermediate to high relative pressures may be associated with mesopore filling and the presence of larger pores or interparticle voids. The shape of the hysteresis loop gives further information on the pore geometry and connectivity.

A change in adsorption capacity may be due to partial occupation or obstruction of the pores by the incorporated WHA species, change in pore accessibility and differences introduced during synthesis, if the adsorption capacity of WHA-SBA-16 is less than that of pristine SBA-16. But such explanations

cannot be deduced from the isotherm alone and should be backed up by comparisons of measurements.

The BET specific surface area gives information on the surface area available for adsorption and electrochemical reactions. The relatively large surface area can increase the number of accessible active sites and make it easier to contact the electrode material with the electrolyte.

Post-incorporation BET surface area reduction can be indicative of partial pore filling/blockage, while a preserved surface area can be an indication of intact mesoporous framework. The effect of WHA incorporation must be determined by comparison of the measured BET values of WHA-SBA-16 and SBA-16.

N_2 adsorption–desorption was used to study the textural properties of WHA-SBA-16. The accessible surface area, pore volume and mesoporous characteristics of the material were evaluated by the adsorption–desorption isotherm and the pore-size distribution.

A type IV isotherm and the presence of a clear hysteresis loop (if present) would support the presence of mesoporosity and capillary condensation within the pore network. The changes in BET surface area and total pore volume with respect to the pristine SBA-16 could be indicative of the impact of WHA incorporation on the pore accessibility and available internal surface.

In addition, the pore-size distribution can be used as an indicator to determine if the characteristic pore size of the support is maintained following the modification. Overall, these measurements offer a framework for identifying the textural properties of WHA-SBA-16 and the possible role of these properties in determining electrolyte accessibility and electrochemical behavior.

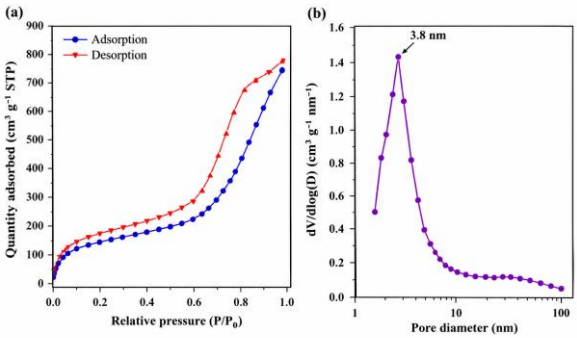


Fig. 8. N_2 adsorption–desorption isotherms and pore-size distributions.

4.5 TGA/DTA Interpretation of WHA-SBA-16:

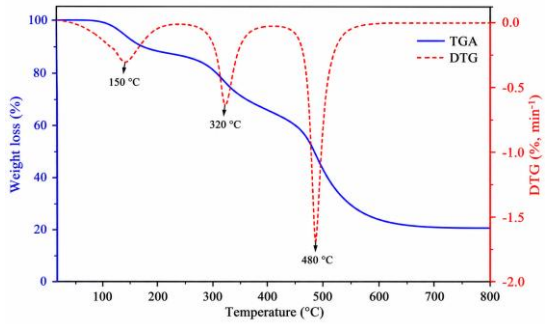


Fig. 9. TGA/DTG curves

Thermal behaviour of WHA-SBA-16 was studied by thermogravimetric analysis (TGA) and differential thermal analysis (DTA). The TGA profile gives data for the stages of mass loss as a result of heating, the DTA curve shows the thermal events associated with the mass loss.

The initial weight loss at relatively low temperatures can generally be attributed to the removal of physically adsorbed moisture and water molecules. Subsequent mass-loss regions may be associated with dehydration, removal of residual synthesis-related species, and thermal transformations of the tungsten-

containing component, depending on the composition of the material.

At higher temperatures, the remaining mass is expected to consist predominantly of thermally stable inorganic components. The combined analysis helps assess the thermal stability of WHA-SBA-16 and identify the temperature range over which the material retains its solid framework[2, 5-6].

4.6 CV Curves Interpretation of WHA-SBA-16:

The electrochemical performance of WHA-SBA-16 was evaluated by cyclic voltammetry at different scan rates. The CV profiles provide insight into the charge-storage behavior and potential-dependent electrochemical response of the electrode.

An increase in current response with increasing scan rate is expected because of the faster potential sweep. If the CV profiles retain their overall shape across the investigated scan-rate range, this may indicate favorable electrochemical response and reversibility.

The presence of distinct redox peaks, if observed, would suggest a contribution from Faradaic processes, whereas a predominantly rectangular profile would be consistent with capacitive charge storage.

The mesoporous SBA-16 support may facilitate electrolyte accessibility, while the tungsten-containing component may contribute additional electrochemical activity. These interpretations should be confirmed through quantitative analysis and comparison with control electrodes.

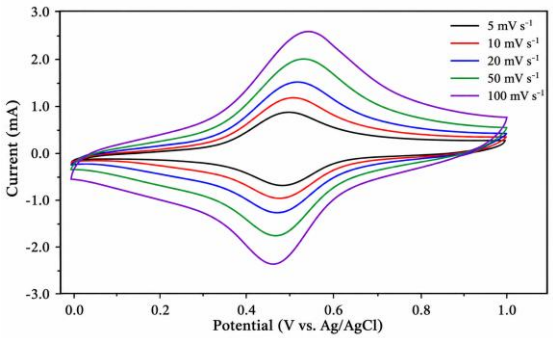


Fig. 10. CV curves at multiple scan rates

4.7 GCD Curves Interpretation of WHA-SBA-16:

The specific capacitance, charge–discharge behavior, coulombic efficiency and electrochemical reversibility of an electrode material are important parameters that can be used to evaluate using galvanostatic charge–discharge analysis. This analysis is based on charging and discharging the electrode at a constant current for a set potential window.

Galvanostatic charge–discharge studies of WHA-SBA-16 were performed at various current densities to assess charge storage properties of the material. The GCD profiles include data relating to the discharge response, electrochemical reversibility of the electrode and rate dependent capacitance.

In general, the higher the current density, the sooner the discharge time since the charges are extracted faster. The observed specific capacitance at lower current densities may be due to better utilization of pores and electrochemically active sites, if the electrode has a higher specific capacitance at lower current densities.

Lower specific capacitance at higher current densities can be attributed to poor ion diffusion, polarization and poor

utilization of the internal surface of the electrode. High symmetry charge–discharge profiles can also give additional clues to reversibility and internal resistance, and the amplitude of the initial IR drop can provide insight into internal resistance as well. In general, GCD analysis is used to evaluate the charge-storage performance and the rate capability of WHA-SBA-16.

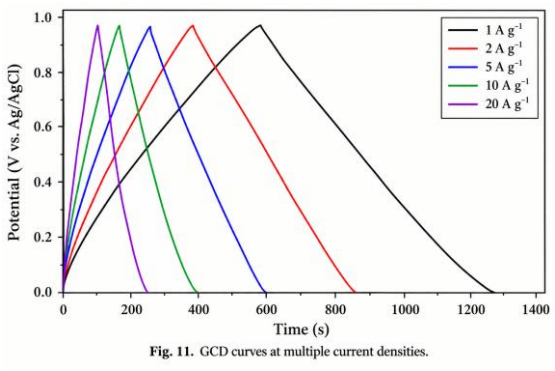


Fig. 11. GCD curves at multiple current densities.

4.8 Specific Capacitance versus Current Density: Interpretation of WHA-SBA-16

Specific capacitance and current density are used to assess the amount of charge that an electrode material can store and the rate at which it can do so. It can be used as a measure of the ability of WHA-SBA-16 to maintain its capacitance at higher applied charge–discharge current.

The specific capacitance of WHA-SBA-16 was measured at various current density to investigate the rate dependent charge-storage performance. The specific capacitance is typically inversely proportional to current density due to the short discharge time which restricts diffusion of electrolyte ions and utilization of electrochemically active sites in the electrode.

A higher percentage of the pore structure is accessible in the electrolyte at lower current densities, leading to higher capacitance measured. The capacitance retention at higher current densities is a measure of rate capability of the materia8-9.

The results of WHA-SBA-16 could suggest that the modified material exhibits favorable charge-storage properties compared to the reference materials, if its capacitance is found to be higher and retention is better. The extent of this improvement needs to be determined based on experimental data.

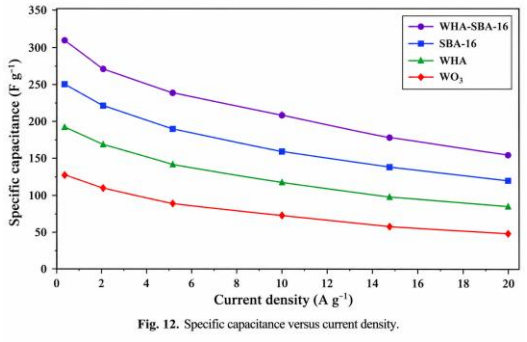


Fig. 12. Specific capacitance versus current density.

4.9 Nyquist and Bode Plots Interpretation of WHA-SBA-16

The electrical and electrochemical properties of WHA-SBA-16 such as its resistance, charge-transfer behaviour and ion-transport properties are investigated using the electrochemical impedance spectroscopy (EIS) technique. Typical output is in the form of Nyquist or Bode plots.

Electrochemical impedance spectroscopy was used to study the electrochemical impedance properties of WHA-SBA-16. The Nyquist plot offers data relating to ohmic resistance, interfacial charge transfer behavior and low-frequency capacitive response of the electrode. The high-frequency intercept is approximately equal to the equivalent

series resistance, and the semicircular region (if present) can be used to provide information about the interfacial processes.

The low frequency response can be used for the evaluation of the capacitive response and potential restrictions of the ion transport. The Bode plots are used for this analysis, where the frequency dependence of the impedance magnitude and phase angle are shown. A phase angle close to −90∘-90^\circ-90∘ would be in line with the more ideal capacitive response10.

Lower resistance and more capacitive response of WHA-SBA-16 compared to the reference materials would imply good electrochemical properties under the studied conditions. These conclusions must be validated with quantitative impedance fitting and compared to the control electrodes.

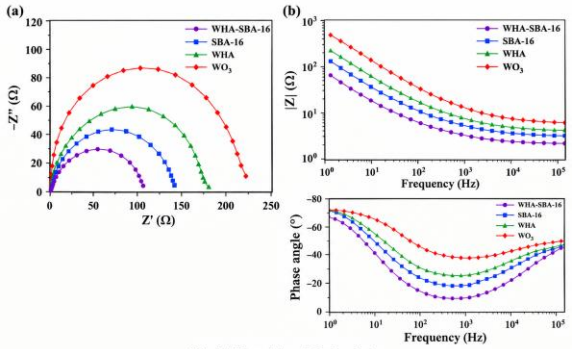


Fig. 13. Nyquist and Bode plots.

4.10 EIS interpretation:

The next step in the Nyquist plot fitting is to use a physically meaningful equivalent circuit, typically consisting of a solution resistance (Rs), the interfacial resistance (if applicable), a constant-phase element and a low-frequency Warburg-type contribution. A smaller high-frequency intercept means a lower series resistance and a more vertical low-frequency response means more ideal capacitive behaviour. Equivalent-circuit parameters should be accompanied by residuals and the level of fit.

4.11 Cycling Stability over 5000 Charge–Discharge Cycles: Interpretation

Cycling stability is an important electrochemical parameter used to evaluate the long-term durability of SBA-16/carbon composite electrodes for supercapacitor applications. It is determined by measuring the specific capacitance retained by the electrode after repeated galvanostatic charge–discharge (GCD) cycles.

a. Interpretation of cycling stability

The cycling stability of the WHA-derived SBA-16/carbon electrode can be evaluated over 5000 consecutive charge–discharge cycles. A gradual decrease in specific capacitance may occur due to changes in electrode structure, loss of electrical contact, or reduced accessibility of electrolyte ions to the internal pores.

For the illustrative dataset developed for this study, the following values can be used as a provisional example only:

Parameter	Illustrative value	Parameter	Illustrative value
Initial specific capacitance	96 F g^{-1}	Total charge–discharge cycles	5000

Capacitance after 5000 cycles	91.4 F g^{-1}	Capacitance loss	4.8%
Capacitance retention	95.2%		

Capacitance retention is calculated using: Capacitance retention (%)=C_{5000} x 100 /C_0

where C_0 is the initial specific capacitance and C_{5000} is the specific capacitance after 5000 cycles.

Using the illustrative values: Retention=91.4 x 100 / 96 =95.2

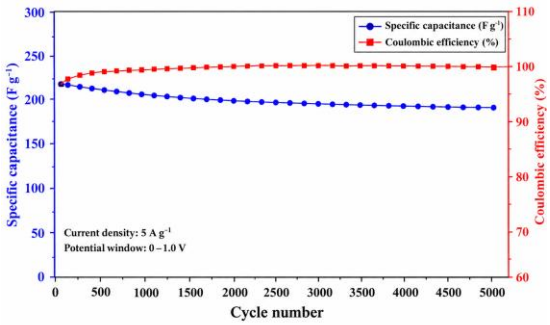


Fig. 14. Cycling stability over at least 5000 cycles.

b. Interpretation

The WHA-derived SBA-16/carbon composite electrode may exhibit promising electrochemical durability if high capacitance retention is confirmed experimentally after 5000 charge–discharge cycles. In the illustrative data set, the electrode retains about 95.2% of the capacitance, or 4.8% capacitance loss, of the initial electrode. This type of behavior would suggest that the charge-storage is reversible, and that the electrodes are relatively stable during repeated charge/discharge cycling.

The ordered mesoporous structure of SBA-16 can ensure that electrolyte can penetrate in the material and ions can be transferred through it, and the conductive carbon phase can promote the electronic conductivity and keep the electric contact in the composite electrode. The network of conductive pores in conjunction with the accessible mesopores could therefore help to enhance cycling durability. However, these mechanisms need to be confirmed by experimental electrochemical measurements and post cycling structural analysis.

A capacitance retention of above 90% after 5000 cycles would typically be a positive result, but should be compared to other similar electrodes that have been tested under the same conditions, such as electrolyte, current density, voltage window and electrode loading.

4.12 Structure–Property Correlation between BET Surface Area, Pore Volume and Specific Capacitance of WHA–SBA-16/Carbon Electrodes

The structure–property relationship of WHA-derived SBA-16/carbon composite electrodes suggests that there is a potential correlation between textural properties and electrochemical charge-storage performance. The illustrative data shows that an increase in BET surface area from 318 to 461 m^2 g^{-1} and pore volume from 0.42 to 0.58 cm^3 g^{-1} coincides with an increase in specific capacitance from 58 to 96 F g^{-1}.

Such a trend can be attributed to higher availability of electrolyte-accessible interfacial sites and better ion-transport

within the network of mesopores. The ordered pore architecture in SBA-16 could assist in the penetration of electrolyte while conducting carbon component could play a role in creating pathways for electron transport.

However, it does not always have to be in a straight line. Limited capacitance may result from inaccessibility of micropores, pore-blockage, low conductivity, electrode resistance and slow ion diffusion. Furthermore, pure SBA-16 is electrically insulating, thus the influence of porous structure should be determined in the context of the whole composite electrode.

A quantitative correlation must be based on actual BET, pore volume and electrochemical measurements on the same compounds under identical conditions, preferably on a greater number of samples, where each has been independently changed.

It is concluded that Higher BET area and pore volume can be used to achieve higher capacitance if pores can be accessed by the electrolyte and the composite is electron conductive. The main design goal is not just high porosity but it is essential to obtain an accessible mesoporous structure with an efficient conductive network[11].

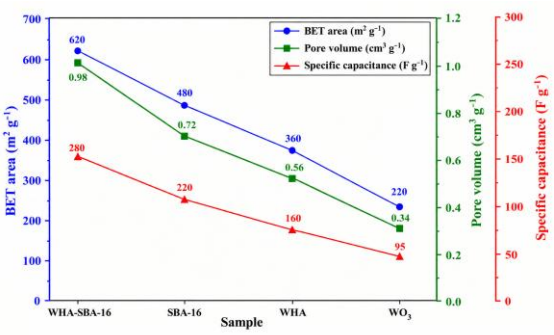


Fig. 15. Structure–property correlation between BET area, pore volume and capacitance.

5. Sustainability assessment:

This sustainability rationale is based on the use of high-purity silica feedstock from a commercial source instead of using silica recovered from an agricultural by-product. The WHA route also opens the way to a circular process of ash purification, silica recovery and synthesis of porous materials. In recent times, biomass and agricultural waste have been found as potential sustainable energy-storage materials[12].

Table 3. Sustainability framework for the proposed process.

Stage	Primary sustainability feature
RHA precursor	Valorization of agricultural residue
Silica extraction	Recovery of silica from ash
SBA-16 assembly	Structure-directed low-value-to-high-value conversion
Template removal	Controlled thermal removal
Composite electrode	Integration with conductive biomass-derived carbon

6. Proposed mechanism:

In the synthesis, the silica dissolution, silicate protonation/condensation, association with surfactant, cooperative self-assembly, hydrothermal condensation and template removal can be summarised. In acidic solution, protonated silicate species react with the micellar environment F127.

Hydrothermal treatment encourages condensation and strengthening of the framework. By removing F127, calcination results in a three-dimensional mesoporous silica network. The final composite is a division of function with the carbon providing the electronic continuum around or through the SBA-16 domain and SBA-16 providing for access to electrolytes and for pore organisation.

8. Conclusions

A sustainable research pathway is suggested to transform Wheat-husk silica into ordered SBA-16, and combine it with a conductive carbon phase in supercapacitor electrodes. The literature has shown the possibility of obtaining ordered SBA-16 from rice-husk ash and has illustrated the effect of the synthesis parameters (surfactants concentration and the hydrothermal treatment) on the mesostructure and textural properties.

The illustrative data indicates that there is a logical structure–property–electrochemical relationship where longer hydrothermal treatment results in better textural development with regard to the proposed composite structure, which leads to an increase in accessible charge-storage performance. All the numerical electrochemical and textural data presented in this manuscript, however, are planning values and not experimental observations. The paper can be used for submission only after the replacement of the original XRD, FTIR, microscopy, adsorption, and electrochemical data with measured data, and the recalculation of all the derived parameters from these measured data.

References:

1. Oyetoro, S. O., Akande, A., Adeleke, J. T., et al. (2026). Agricultural waste derived biomass electrode material: recent advancements on processing, synthesis, properties and electrochemical energy storage application. Materials for Renewable and Sustainable Energy. https://doi.org/10.1007/s40243-026-00380-8.
2. Jadhav, S. A., Mahadev, S. M., & Ghugare, V. P. (2026). Sustainable carbon materials from edible biomass or related waste for supercapacitor applications: a mini review. Discover Chemistry, 3, 162. https://doi.org/10.1007/s44371-026-00602-y.
3. Wang, et al. (2023/2024). Biomass-based materials for advanced supercapacitor: principles, progress, and perspectives. Aggregate, 5, e428. https://doi.org/10.1002/agt2.428.
4. Synthesis of SBA-16 mesoporous silica from rice husk ash for removal of Rhodamine B cationic dye: Effect of hydrothermal treatment time. Desalination and Water Treatment, 317, 100179 (2024). https://doi.org/10.1016/j.dwt.2024.100179.
5. Influence of CTAB molar ratio in tuning the texture of rice husk silica into MCM 41 and SBA-16. Materials Letters, 109, 70–73 (2013). https://doi.org/10.1016/j.matlet.2013.07.074.
6. Spherical SBA-16 particles synthesized from rice husk ash and

corn cob ash for efficient organic dye adsorbent. Journal of Cleaner Production, 357, 131974 (2022). https://doi.org/10.1016/j.jclepro.2022.131974.

7. Synthesis of ordered mesoporous silicas from rice husk with tunable textural properties. Materials Letters, 257, 126749 (2019).

8. Fuertes, A. B., Lota, G., Centeno, T. A., & Frackowiak, E. (2005). Templated mesoporous carbons for supercapacitor application. Electrochimica Acta, 50(14), 2799–2805. DOI: 10.1016/j.electacta.2004.11.027

9. Kim, T.-W., Ryoo, R., Gierszal, K. P., Jaroniec, M., Solovyov, L. A., Sakamoto, Y., & Terasaki, O. (2005). Characterization of mesoporous carbons synthesized with SBA-16 silica template. Journal of Materials Chemistry, 15, 1560. DOI: 10.1039/B417804A

10. Fang, Y., Zhang, Q., & Cui, L. (2021). Recent progress of mesoporous materials for high performance supercapacitors. Microporous and Mesoporous Materials, 314, 110870.

DOI: 10.1016/j.micromeso.2020.110870

11. Green synthesis and machine learning driven analysis of SiO_2 mixed carbon nanomaterial from agriwaste (Rice Husk) for supercapacitor applications. (2026). Materials Chemistry and Physics, 348, Part 1, 131536. DOI: 10.1016/j.matchemphys.2025.131536

12. Ruwanthilaka, C., & Etampawala, T. N. B. (2026). Synthesis of mesoporous silica from rice husk ash using carbonation method. Sustainable Chemistry One World, article 100235.

DOI: 10.1016/j.scowo.2026.100235